

## Triphenylmethane Dye Activation of Beta-Arrestin

Larry S. Barak,\*<sup>#</sup> Yushi Bai,<sup>#</sup> Joshua C. Snyder,<sup>#</sup> Jiangbo Wang,<sup>§</sup> Wei Chen,<sup>§</sup> and Marc G. Caron\*,<sup>#,†,§</sup>

\*Departments of Cell Biology, <sup>†</sup>Neurobiology, and <sup>§</sup>Medicine, Duke University, Durham, North Carolina 27710, United States

 [Supporting Information](#)

**ABSTRACT:**  $\beta$ -Arrestins regulate G protein-coupled receptor signaling as competitive inhibitors and protein adaptors. Low molecular weight biased ligands that bind receptors and discriminate between the G protein dependent arm and  $\beta$ -arrestin, clathrin-associated arm of receptor signaling are considered therapeutically valuable as a result of this distinctive pharmacological behavior. Other than receptor agonists, compounds that activate  $\beta$ -arrestins are not available. We show that within minutes of exposure to the cationic triphenylmethane dyes malachite green and brilliant green, tissue culture cells recruit  $\beta$ -arrestins to clathrin scaffolds in a receptor-activation independent manner. In the presence of these compounds, G protein signaling is inhibited, ERK and GSK3 $\beta$  signaling are preserved, and the recruitment of the beta2-adaptin, AP2 adaptor complex to clathrin as well as transferrin internalization is reduced. Moreover, malachite green binds  $\beta$ -arrestin2-GFP coated immunotrap beads relative to GFP only coated beads. Triphenylmethane dyes are FDA approved for topical use on newborns as components of triple-dye preparations and are not approved but used effectively as aqueous antibiotics in fish husbandry. As possible carcinogens, their chronic ingestion in food preparations, particularly through farmed fish, is discouraged in the U.S. and Europe. Our results indicate triphenylmethane dyes as a result of novel pharmacology may have additional roles as  $\beta$ -arrestin/clathrin pathway signaling modulators in both pharmacology research and clinical therapy.



G protein-coupled receptors (GPCRs) bind arrestin proteins after receptor activation by agonists and phosphorylation by G protein-coupled receptor kinases. Arrestin binding produces a termination of G-protein signaling, and until very recently, arrestins were considered only for their role as GPCR signal transduction desensitizers.<sup>1</sup> In the past decade, we have come to appreciate that arrestins orchestrate a number of intracellular signaling paradigms that occur independent of G protein participation. Activated arrestin2 and 3 (also known as  $\beta$ -arrestin1 and  $\beta$ -arrestin2, respectively) direct desensitized receptors to clathrin-rich plasma membrane, where together they organize molecular signaling scaffolds.<sup>2,3</sup>  $\beta$ -Arrestin dependent signal transduction includes protein kinases, for instance, Src and AKT/GSK3 $\beta$ ; involves transcription factor regulation through associated kinases such as ERK and JNK; and regulates diverse cellular behaviors such as adaptation, proliferation, and apoptosis.<sup>2,4</sup> As a consequence of the dichotomy in receptor signaling arising from G protein and  $\beta$ -arrestin pathways, searches are underway for receptor biased pathway modulators that could provide drugs with novel therapeutic profiles.<sup>5</sup>

$\beta$ -Arrestin fusion proteins make practical, optically detectable sensors for identifying GPCR ligands, and its green fluorescent protein (GFP) fusion finds use in high content screening assays.<sup>6</sup> For example, within seconds to minutes of receptor exposure to agonist, receptor complexed  $\beta$ -arrestin-GFP can be imaged in clathrin coated pits.<sup>6,7</sup> This remarkably simple readout also provides an accurate indication of both receptor and  $\beta$ -arrestin activation. As a prelude to a Molecular Libraries Probe Centers Network (MLPCN)  $\beta$ -arrestin based, ultrahigh throughput screen for small molecule nonpeptide agonists of the neuro-

tensin1 receptor (NTR1),<sup>8</sup> we performed using a U2OS cell line permanently expressing NTR1 and  $\beta$ -arrestin2-GFP a 5  $\mu$ M screen of the Johns Hopkins FDA-drug library.<sup>9</sup> Similar to how  $\beta$ -arrestin regulates GPCR behavior in general, activated neurotensin receptor, NTR1,  $\beta$ -arrestin signaling complexes form clathrin-based plasma membrane and endocytic aggregates (Figure 1A, left lower panel).<sup>6,10</sup> We observed a similar neurotensin-like response for two wells in the Hopkins Library screen that corresponded to Brilliant Green (BG) and Triple-Dye (BG, Gentian Violet and Proflavine hemisulfate; 2:2:1 by weight).

Brilliant Green and Gentian Violet are members of the large triphenylmethane dye family (Figure 1B, right panel) and are primarily utilized as coloring agents.<sup>11–14</sup> Triphenylmethane dyes, however, are also utilized extensively outside the textile industry. They find laboratory use as fluorescent biosensors<sup>15–17</sup> and as therapeutics, particularly in fish farming to treat bacteria, fungal, and parasitic infections.<sup>13,14</sup> Despite the proven bioactivity of triphenylmethane derivatives, direct BG activation of  $\beta$ -arrestin appeared unlikely given the historical absence of direct small molecule  $\beta$ -arrestin activators and the complex regulation that  $\beta$ -arrestins undergo with receptors;<sup>1,2</sup> and indeed our findings could simply be a direct consequence of identifying a new, albeit remarkable, small molecule agonist for the NTR1. Therefore, in an attempt to determine the role of BG in  $\beta$ -arrestin activation, we investigated  $\beta$ -arrestin recruitment for a cohort of

**Received:** February 19, 2013

**Revised:** July 18, 2013

**Published:** July 18, 2013

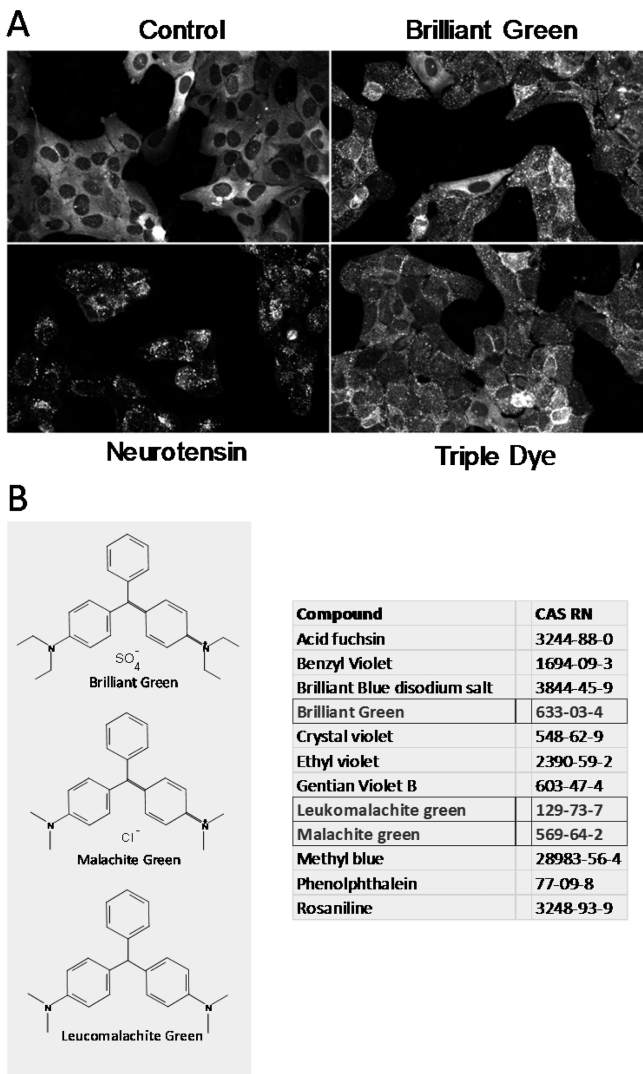


**Figure 1.** Fluorescence images of U2OS cells from a high-content screen searching for NTR1 agonists. (A) Cells expressing the human HA-NTR1 receptor and a  $\beta$ -arrestin2-GFP reporter exposed to vehicle (upper left panel), neurotensin peptide (lower left panel), Brilliant Green (upper right panel), or Triple-Dye (lower right panel). (B) Table and structures of representative triphenylmethane compounds along with their CAS registration numbers.

G protein-coupled receptors that were exposed to BG, the industrially important dye Malachite Green (MG), and the reduced, uncharged metabolite of MG, Leukomalachite Green (LG) (Figure 1B).

## MATERIALS AND METHODS

**Plasmids and Cells.** Human neurotensin receptor 1 (NTR1) and N-terminal triple hemeagglutinin-tagged neurotensin receptor 1 (3HA-NTR1) in pcDNA3.1+ were purchased from the Missouri S&T cDNA Resource Center (Rolla, MO). The GFP conjugate of the human 3HA-NTR1 was generated by PCR with the receptor inserted in frame at the Nhe I/BamH I restriction sites of pEGFP-N3 (Clontech, Mountain View, CA). Mitochondria targeted apo-aequorin was a gift from Dr. Stanley Thayer (University of Minnesota, Minneapolis, MN). The GloSensor-22F cAMP Plasmid was purchased from Promega (Madison, WI). U2OS stable cells expressing  $\beta$ -arrestin2-GFP and receptor were provided by our laboratory from the cell stocks

which are part of the Duke University National Institutes on Drug Abuse (NIDA) P30 Center, [www.duke.edu/web/gpcr-assay/index.html](http://www.duke.edu/web/gpcr-assay/index.html). HEK293 cells stably expressing GFP- $\beta$ 2adap tin were generated as described.<sup>18</sup>

**Antibodies.** Anti-HA mouse monoclonal antibody was isolated in house using the hybridoma clone X22 from the American Type Culture Collection (Manassas, VA). AlexaFluor 568 goat antimouse antibody and Alexa-Fluor 680 goat antimouse IgG were purchased from Invitrogen (Carlsbad, CA). IR-Dye 800 conjugated antirabbit IgG was from Rockland Antibodies and Assays (Gilbertsville, PA). The phospho-p44/42 MAPK (ERK1/2) (Thr202/Tyr204) (197G2) rabbit mAb, p44/42 MAPK (ERK1/2) (3A7) mouse mAb, antiphospho-GSK-3 $\alpha$ / $\beta$  Ser-21/9, and GSK-3 $\alpha$ / $\beta$  (D7S3) XP rabbit mAb were purchased from Cell Signaling Technology (Beverly, MA).

**Automated High-Throughput Screening.** U2OS cells stably expressing NTR1 and  $\beta$ -arrestin2-GFP were split into MGB101-1-2-LG glass-bottom 384-well plates (MatriCal, Spokane, WA) using a Multidrop 384 liquid dispenser (Thermo Scientific, Hudson, NH). Each well contained 25- $\mu$ L aliquots of 12 000 cells in Minimum Eagle's medium (MEM) containing 10% fetal bovine serum (FBS) and 100 U/mL penicillin/streptomycin (Life Technologies, Grand Island, NY). The plates were incubated overnight at 37 °C in 5% CO<sub>2</sub>, and on the following day the media was changed to 30  $\mu$ L clear MEM without serum. Compounds at 50  $\mu$ M in 5% DMSO from the Johns Hopkins FDA-drug Library were added to each well using a MicroLab StarLET liquid handler (Hamilton Robotics, Reno, NV) and diluted 10-fold to 5  $\mu$ M final concentration. The plates were returned to the incubator for 40 min, and the cells were fixed by adding 30  $\mu$ L of 2% paraformaldehyde-phosphate buffered saline (PBS) to each well. Plates were stored at 4 °C until analysis on an ImageXpress Ultra (Molecular Devices, Sunnyvale, CA) at 488 nm. Images were analyzed using a wavelet algorithm to measure formation of fluorescence aggregates.<sup>19</sup> Image results were also visually confirmed.

**Microscope Imaging.** For dose response assays of the triphenylmethane dyes, U2OS cells stably expressing  $\beta$ -arrestin2-GFP with or without various GPCRs were plated into glass-bottom 384-well plates at 95–100% cell confluence. Cells were treated with a serial concentration of dye compounds or known agonists for 40 min, fixed in paraformaldehyde, and examined on a Zeiss Axiovert200 fluorescent microscope platform using a plan-apochromat 40 $\times$ /0.95 N.A. air objective. For confocal microscope imaging on a Zeiss LSM-510, cells were plated at a density of (4–8)  $\times$  10<sup>4</sup>/well in 35 mm MatTek (Ashland, MA) glass coverslip dishes. Transient transfection or immunostaining staining was performed as described.<sup>20</sup> Cells were examined with a 100 $\times$ /1.4 N.A. oil objective at 488 nm excitation for the GFP tag and 568 nm for AlexaFluor 568 labeled antibody. Images were analyzed using a wavelet algorithm,<sup>19</sup> and data were analyzed using Prism 5.0 software (GraphPad, San Diego, CA).

**Neurotensin Receptor Internalization Assay.** U2OS cells stably expressing 3HA-NTR1 and  $\beta$ -arrestin2-GFP were grown until confluent on poly-D-lysine coated 96-well plastic culture plates (Corning, Corning, NY). The cells were serum-starved for 5 h in clear MEM before treatment with a serial concentration of neurotensin or Brilliant Green in clear MEM with 10 mM HEPES at 37 °C for 40 min. The detection of remaining 3HA-NTR1 on the cell surface was performed following the protocol of Daigle, et al. (2007) with modifications. Briefly, cells were fixed with 4% paraformaldehyde at room temperature for 20 min, washed once in PBS (without detergent to avoid membrane

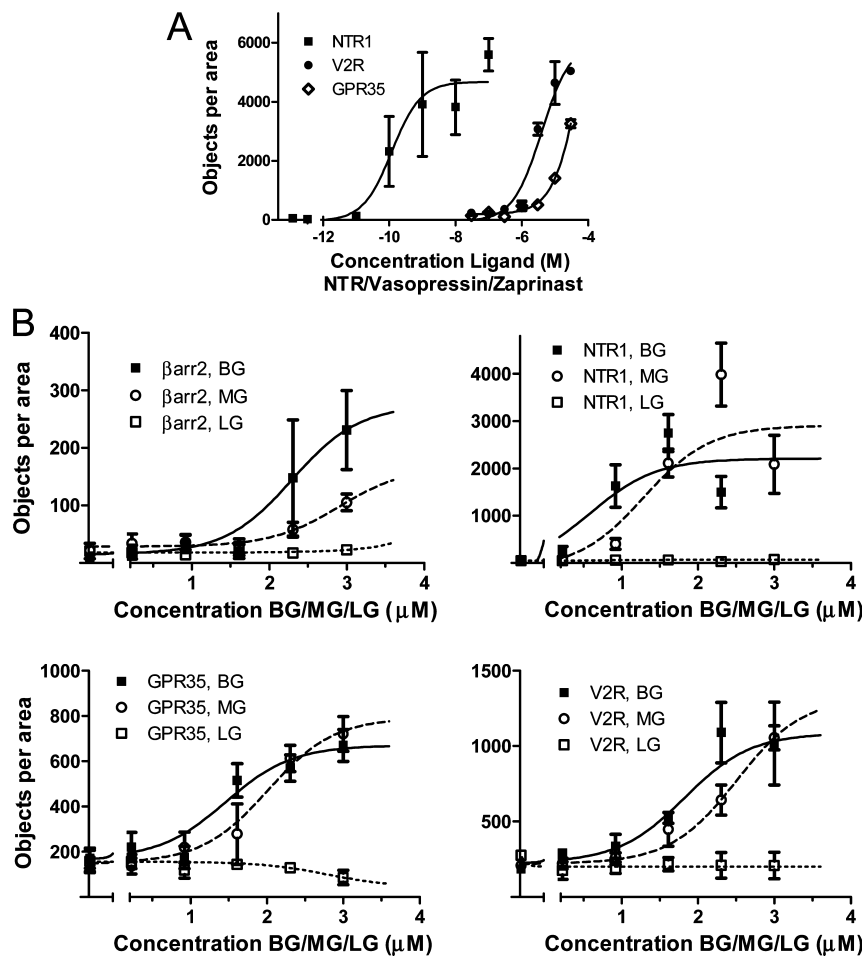


**Figure 2.**  $\beta$ -Arrestin activation by triphenylmethane dyes. (A) Responses of transfected cells, in objects per unit area, that were incubated with the cognate receptor agonists zaprinast (GPR35),<sup>21</sup> vasopressin (V2R),<sup>22</sup> or neurotensin (NTR1). (B) Graphs depicting the formation of  $\beta$ -arrestin-GFP fluorescent aggregates in the same cell lines resulting from exposure to triphenylmethane compounds. The U2OS cell lines each permanently expressing  $\beta$ -arrestin-GFP and no transfected receptor (control), NTR1, GPR35, and V2R were treated with the three compounds BG/MG/LG. Image data (as objects, mean  $\pm$  SEM) corresponding to the graphs were obtained with a Zeiss Axiovert 200 fluorescence microscope equipped with a plan-apochromat 40 $\times$ /0.95 air objective and were analyzed using a wavelet based algorithm<sup>19</sup> ( $N = 3$ ).

permeabilization), blocked in LI-COR Odyssey blocking buffer for 90 min, and incubated with anti-HA mouse monoclonal antibody overnight at 4 °C. After three washes in Tris-buffered saline containing 0.1% Tween-20, AlexaFluor 680 goat antimouse IgG was added to assess immunoreactivity. Immunofluorescence was quantified on the Odyssey Infrared Imager (LI-COR Biotechnologies, Lincoln, NE) set at a 169 mm resolution, a focus offset of 3, and an intensity of 5. Data were fit using Prism 5.0 software.

**Western Blot Analysis.** U2OS cells stably expressing  $\beta$ -arrestin2-GFP with or without GPR35, NTR1, or V2R were seeded onto six-well plates and grown until 90% confluent at 37 °C in 5% CO<sub>2</sub>. The cells were serum-starved overnight in MEM prior to the experiment. The cells were then stimulated as indicated at 37 °C. Supernatants were discarded and cells were lysed with 150  $\mu$ L/well lysis buffer containing proteinase and phosphatase inhibitors (Roche and Thermo Scientific). Cells were further disrupted by sonication. Supernatants were collected by centrifuge and boiled in SDS Sample Buffer for 5 min. The protein samples were subjected to SDS-PAGE using 10% Novex Tris-Glycine Gels (Invitrogen), transferred to nitrocellulose membranes (Bio-Rad Laboratories, Hercules, CA), blocked with 5% nonfat milk powder in Tris-buffered

saline containing 0.2% Tween-20 for 1 h, followed by incubation with primary antibodies and then an IR-Dye 800 conjugated antirabbit IgG. Imaging and quantification of bands were performed on the LI-COR Odyssey. Data were analyzed using Prism 5.0.

**Apo-Aequorin Calcium Measurement.** HEK293 cells plated in 100-mm dishes were transiently transfected with 0.2  $\mu$ g of human NTR1 cDNA and 10  $\mu$ g of apo-aequorin cDNA using a calcium phosphate protocol. After 4–6 h, the cells were detached and plated into a 96 well, white OptiPlate (PerkinElmer; Waltham, MA). The following day cells were equilibrated with 5  $\mu$ M Coelenterazine-h (Promega) at 37 °C for 1 h and 50 min. To assess effects of compound pretreatment, the cells were exposed to either a dye compound or neurotensin for a further 10 min. Bioluminescence was detected immediately upon injection of 10 nM neurotensin into each well with a Mithras LB940 luminescence reader running MikroWin2000 software (Berthold Technologies, Oak Ridge, TN). To assess compound responsiveness, a 96-well assay plate with 2X concentration of dye compounds or neurotensin in PBS with calcium and magnesium was prepared. A transfected 1 mL suspension of cells (equivalent to one 100-mm dish) in 10% FBS-MEM was equilibrated in a dark 37 °C incubator with 5  $\mu$ M coelenterazine-

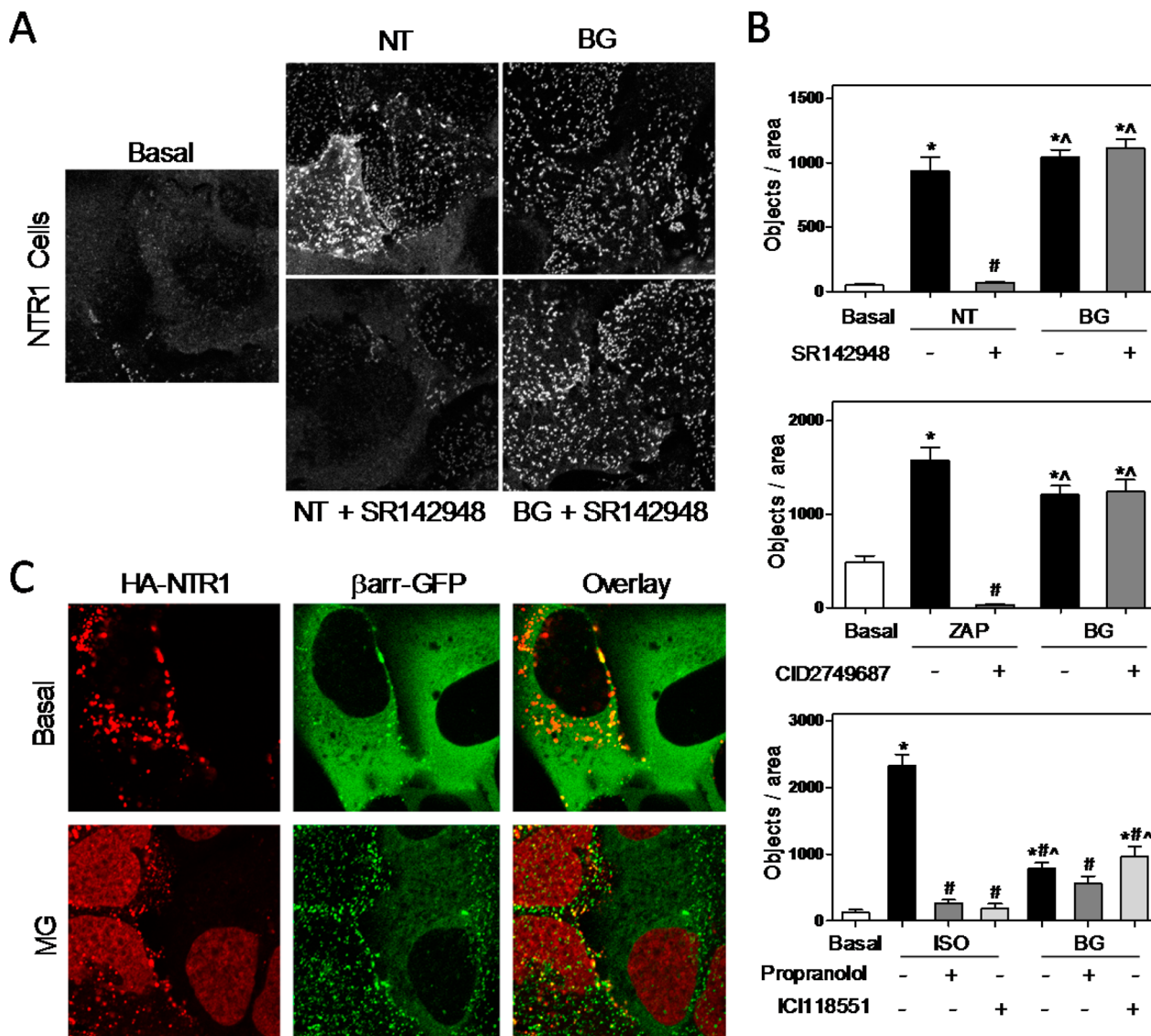


**Figure 3.** Receptor conformation in the activation of  $\beta$ -arrestin by Brilliant Green. (A) Fluorescence images of U2OS cells expressing  $\beta$ -arrestin2-GFP and HA-NTR1 exposed to either NT or BG in the absence (upper panels) and presence (lower panels) of the NTR1 antagonist SR142948A ( $10 \mu\text{M}$ ). The leftmost panel shows an untreated control. Images were obtained on a Zeiss LSM510 confocal microscope using a  $100\times/\text{NA } 1.43$  plan apochromat objective. (B) Quantification of  $\beta$ -arrestin fluorescence aggregates in confocal images obtained in (A) for the NTR1 and also those obtained from similar images in analogous experiments for  $\beta$ -arrestin2-GFP permanent U2OS cell lines expressing either HA-GPR35 or  $\beta$ 2AR. Each receptor type was pre-exposed to  $1-10 \mu\text{M}$  of a cognate antagonist or inverse agonist SR142948A ( $10 \mu\text{M}$ , NTR1), CID2745687 ( $1 \mu\text{M}$ , GPR35), and propranolol or ICI118551 ( $10 \mu\text{M}$ ,  $\beta$ 2AR) for 15 min at  $37^\circ\text{C}$  followed by addition of its cognate agonist ( $0.5 \text{ nM}$  NT,  $1 \mu\text{M}$  Zaprinast,  $1 \mu\text{M}$  isoproterenol) or BG ( $3-5 \mu\text{M}$ ).  $N = 3-5$  experiments and data are mean  $\pm$  SEM and assessed in GraphPad Prism by one-way Anova using Bonferroni's post test (\* vs basal, # vs agonist, ^ vs agonist plus antagonist,  $p < 0.05$ ). (C) Dependence of  $\beta$ -arrestin2-GFP aggregate formation on receptor expression. Control U2OS cells expressing only  $\beta$ -arrestin2-GFP were transiently transfected with HA-tagged NTR1 and treated with either vehicle or  $5 \mu\text{M}$  Malachite Green (MG) for  $40-60$  min at  $37^\circ\text{C}$  and then fixed. HA-tagged receptors were labeled with mouse anti-HA and goat antimouse AlexaFluor 568 antibodies. Receptors and  $\beta$ -arrestin2-GFP were imaged as in (A) at  $488 \text{ nm}/568 \text{ nm}$  ( $N = 3$ ).

h for 2 h using mild agitation. Immediately prior to measurement, the cells were diluted to a concentration of  $1 \times 10^6$  cells per milliliter with culture medium for injection. Bioluminescence for each well was recorded for 30 s post injection.

**GloSensor cAMP Assay.** HEK293 cells in 100-mm dishes were transiently transfected with  $5 \mu\text{g}$  of GloSensor plasmid cDNA and  $2 \mu\text{g}$  of receptor cDNA using a calcium phosphate protocol. After 4–6 h, cells were detached and plated at 50 000 cells/well into clear MEM with 2% FBS, HEPES, and glutamine using poly-D-lysine coated (Sigma), 96-well Costar 3610 (Corning Inc.) assay plates. The following day, cells were washed with Hank's Balanced Salt solution (HBSS, Life

Technologies-GIBCO) and equilibrated in the dark with 4 mM luciferin in HBSS for 2 h at room temperature. Luciferin buffer was removed and  $90 \mu\text{L}$  of HBSS and  $10 \mu\text{L}$  of 10 $\times$  compound was added to each well. Following a 10 min incubation period, bioluminescence was read with an integration time per well of 1.2 s for four sequential plate determinations. To assess the effect of dye compound on luminescence signaling, dose response curves were obtained *in vitro* for luciferase and luciferin in the presence and absence of brilliant green.

**Transferrin Endocytosis.** U2OS cells stably expressing  $\beta$ -arrestin2-GFP with or without overexpressed NTR1 in  $100 \mu\text{L}$  MEM in 96-well plates were pretreated with either  $5 \mu\text{M}$  BG or

10  $\mu$ M MG for the indicated times before 5  $\mu$ M AlexaFluor-680 transferrin (Life Technologies, Grand Island, NY) was added for 40 min at 37 °C. Cells were then washed in MEM and fixed in 4% paraformaldehyde for 20 min at room temperature, and the internalized transferrin was measured at 680 nm excitation on a LI-COR Odyssey Infrared Imaging system.

**$\beta$ -Arrestin2 Binding to Malachite Green.** HEK293 cells in 150-mm dishes were transiently transfected with 20  $\mu$ g of plasmid cDNA expressing either  $\beta$ -arrestin2-GFP, GFP, or empty vector. Lysate preparation: After 24 h, cells were washed with phosphate buffered saline (PBS) and lysed with 1 mL/dish lysis buffer (10 mM Tris-HCl containing 150 mM NaCl, 5 mM EDTA, 0.1% SDS; 1% Triton X-100, and 1% sodium deoxycholate at pH 7.5) and cOmplete protease inhibitor cocktail (Roche Diagnostics, Mannheim, Germany). After a brief sonication on ice, cell lysates (1 mL in eppendorf tubes) were rotated gently at 4 °C for 30 min followed by centrifugation at 20000g at 4 °C for 20 min. Supernatants were transferred to tubes precooled on ice. Bead preparation: Agarose GFP-Trap beads (20–40  $\mu$ L per 150 mm dish) (Chromotek or Allele Biotech, San Diego, CA) were suspended, washed, and then pelleted at 2500g a total of 3 $\times$  in 500  $\mu$ L of ice cold lysis buffer. Cell lysates prepared as above were added to individual tubes of beads, and the lysates were tumbled with the GFP-Trap beads either at room temperature for 2 h or at 4 °C overnight. Each bead slurry sample was then washed three times with 0.5% NP40 in PBS, and then samples from each tube were either (1) incubated with 10  $\mu$ M MG for 30 min at room temperature in preparation for confocal observation or (2) eluted in SDS sample buffer and divided 80/20 for AcquaStain (Bulldog Bio, Portsmouth, NH) gel staining or Western blotting.  $\beta$ -Arrestin2-GFP and GFP were detected in Western blots with primary rabbit antibodies from Abcam (anti- $\beta$ -arrestin2 Catalog No. ab167047 Cambridge, MA) and GeneTex Inc. (anti-GFP, Catalog No. GTX113617, Irvine, CA) at 1:700 and 1:500 dilutions, respectively, followed by application of goat antirabbit secondary antibodies (Rockland Antibodies and Assays, catalog no. 611-132-122, Gilbertsville, PA) at a dilution of 1:5000 for LI-COR Odyssey imaging.

## ■ RESULTS

**Triphenylmethane Dye-Induced  $\beta$ -Arrestin Translocation.** Dose responses for  $\beta$ -arrestin translocation in permanent lines of U2OS cells containing no transfected receptor (control), the NTR1, the pamoic acid receptor (GPR35), and the vasopressin receptor (V2R) are shown for cognate agonists (Figure 2A) and BG, MG, or LG (Figure 2B). The cell lines contain  $\beta$ -arrestin2-GFP with intensity ratios of 1.6/1.2/1.2/1 (NTR1/V2R/GPR35/control = 1). LG has no  $\beta$ -arrestin2 translocation inducing activity in all cell lines and MG is 2–3-fold less potent than BG but is equally efficacious. BG is the most potent  $\beta$ -arrestin2 activator. It induces translocation to levels almost equal to that of neurotensin and surprisingly has activity without an exogenous GPCR present (control, Figure 2B, upper left panel).

**GPCR Role in Triphenylmethane Dye-Induced  $\beta$ -Arrestin Translocation.** In order to characterize the role of the conformational state of the receptor in BG/MG  $\beta$ -arrestin2 activation, we simultaneously treated the NTR1, GPR35, and beta2-adrenergic receptor ( $\beta$ 2AR) expressing U2OS cells with cognate antagonists or inverse agonists (Figure 3A,B, SR142948A for NTR1, CID2745687<sup>21</sup> for GPR35, and propranolol and ICI118551 for the  $\beta$ 2AR) and measured the

aggregation of  $\beta$ -arrestin2-GFP. These antagonists were unable to block BG mediated  $\beta$ -arrestin2 recruitment in contrast to their abilities to inhibit agonist mediated  $\beta$ -arrestin2 recruitment to the cognate receptors.<sup>23</sup> Even though activated receptors were not required for the induction of  $\beta$ -arrestin2-GFP recruitment by BG and MG, we observed that U2OS/ $\beta$ -arrestin2-GFP cells transfected with GPCRs contained more  $\beta$ -arrestin2-GFP aggregates upon exposure to BG and MG (Figure 3C). Thus, at first glance  $\beta$ -arrestin activation in the presence of triphenylmethane dye exposure appears receptor dependent. We investigated this observation by transfecting epitope tagged NTR1 receptors into the control  $\beta$ -arrestin2-GFP U2OS line and visualizing that cells containing transfected NTR1 contained many more  $\beta$ -arrestin-GFP aggregates in response to MG than contiguous cells lacking transfected receptor (Figure 3C lower panels).

**Receptor Absence from MG Activated  $\beta$ -Arrestin/Clathrin Complexes.** The above data indicate that the ability of GPCRs to activate  $\beta$ -arrestin2 in the presence of MG and BG does not require an agonist induced conformational change in the receptor.<sup>1</sup> The ability of MG and BG to induce  $\beta$ -arrestin2-GFP translocation for multiple receptors in the presence of inhibitors, however, indicates that BG and MG do not behave as orthosteric receptor agonists. GPCR agonists typically induce not only receptor internalization but also cluster these  $\beta$ -arrestin/receptor complexes in clathrin rich membrane pits for signaling and recycling by clathrin/AP2 coated vesicles.<sup>1,24</sup> From Figure 4A, it is apparent that 10  $\mu$ M MG treatment results in the activation of  $\beta$ -arrestin2-GFP and its widespread colocalization with clathrin in plasma membrane punctae in cells containing V2R or NTR1. Similar colocalization was also observed for Flag- $\beta$ -arrestin2 (Supporting Information, Figure S1). Measurement of clathrin aggregates in the membrane by immunostaining under basal conditions (in the absence of drugs) demonstrated that cells containing the NTR1 had over twice the number of clathrin positive areas as either the  $\beta$ -arrestin2-GFP control cells or V2R expressing U2OS cells (Supporting Information, Figure S2). However, these receptors, that normally bind  $\beta$ -arrestin2 with high affinity and internalize with it into well recognized “doughnut-shaped” endosomes, do not exhibit this agonist typical behavior in the presence of MG as observed by  $\beta$ -arrestin-GFP fluorescence (Figure 4B, compare upper to lower panels). Therefore, to assess whether a receptor is necessary to form these dye induced complexes with clathrin, we performed colocalization studies using the permanent line of U2OS cells expressing HA-GPR35 and  $\beta$ -arrestin2-GFP (Figure 4C). Application of 10  $\mu$ M of the GPR35 agonist pamoic acid coclusters GPR35 and  $\beta$ -arrestin (rightmost panels), while in contrast the receptor in the presence of 10  $\mu$ M MG is absent from  $\beta$ -arrestin aggregates (middle panels).

**Effect of Triphenylmethane Dyes on Receptor Internalization.** Using NTR1-GFP and HA-epitope tagged NTR1, we investigated both internalization and  $\beta$ -arrestin scaffolding in the presence of the triphenylmethane dyes. In HEK293 cells, NT treatment results in significant NTR1 internalization from the plasma membrane that is visible as endosomes (Figure 5A, mid upper panel). In contrast, there is no BG induced loss of NTR1 from the plasma membrane (Figure 5A, right upper panel); in fact NTR1 plasma membrane receptor levels slightly increase with BG treatment as opposed to NT exposure (middle panels).

**Triphenylmethane Dyes, Clathrin, and AP2.** In the steady state activated receptor/ $\beta$ -arrestin complexes that bind AP2, via  $\beta$ -arrestin directly interacting with the  $\beta$  and  $\mu$  AP2

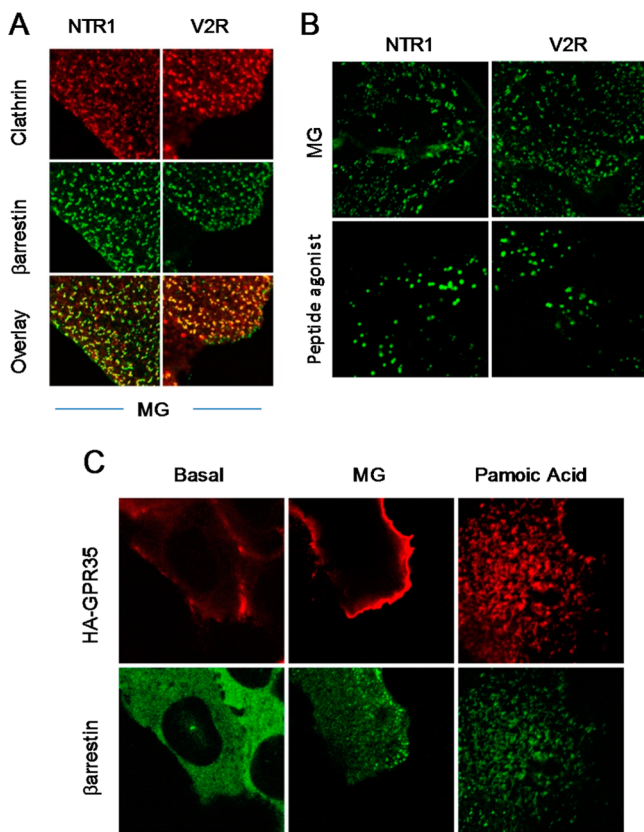


**Figure 4.** Triphenylmethane dye activated  $\beta$ -arrestin complexes. (A) ( $\beta$ -arrestin/clathrin) U2OS cells permanently expressing a transfected receptor, NTR1 or V2R, and  $\beta$ -arrestin2-GFP were treated with 10  $\mu$ M malachite green for 40 min at 37 °C, fixed in 1%PFA, permeabilized with 0.5% Triton X-100 in PBS, treated with a 1:70 dilution of mouse anticlathrin X22 antibody sera, and labeled with a 1:1500 dilution of goat antimouse AlexaFluor 568 secondary antibody. Cells were imaged by confocal microscopy using 488 (GFP)/568 (AlexaFluor) nm excitation. (N = 3). (B) ( $\beta$ -arrestin/endosomes) NTR1 or V2R and  $\beta$ -arrestin2-GFP U2OS cells in MEM were pretreated with 10  $\mu$ M MG for 10 min at 37 °C, exposed to cognate agonist (5 nM NT or 40 mIU vasopressin) for 40 min, and then fixed for confocal imaging. (N = 3). (C) ( $\beta$ -Arrestin/receptor) U2OS cells permanently expressing HA-GPR35 and  $\beta$ -arrestin2-GFP were treated with either 10  $\mu$ M MG or 10  $\mu$ M pamoic acid for 40 min at room temperature and fixed. GPR35 receptors were visualized for confocal imaging using anti-HA mouse primary antibody at 1:400 followed by a 1:1500 dilution of goat antimouse AlexaFluor 568 secondary antibody (N = 3).

subunits, and clathrin, are disassembled and inactivated in acidic endosomes.<sup>1,2,25,26</sup> The accumulation of activated  $\beta$ -arrestin/clathrin complexes and the modest inhibition of basal NTR1 internalization in the presence of BG suggest that the triphenylmethane dyes might be inhibiting  $\beta$ -arrestin trafficking. Therefore, we investigated triphenylmethane dye effects on cells containing AP2 labeled with GFP- $\beta$ 2adaptin. Upon cell exposure to either BG or MG, the number of AP2 vesicles was greatly decreased (Figure 5B). Therefore, the accumulation of  $\beta$ -arrestin/clathrin complexes in the absence of receptor activation is consistent with a BG and MG inhibition of the AP2/clathrin interaction. This is supported by the observation that transferrin internalization is decreased to 76 and 54% of that observed in the control cells after a pre-exposure as brief as 10 or 30 min respectively to 5  $\mu$ M BG or 10  $\mu$ M MG (Figure 5C).

#### Effect of Triphenylmethane Dyes on $\beta$ -Arrestin Related Signaling.

Even though  $\beta$ -arrestin recycling is modified,

arrestin colocalization with clathrin suggests the formation of signaling scaffolds analogous to those observed in the presence of receptor activation but occurring without the active participation of the receptor. Therefore, we evaluated downstream indicators of clathrin/ $\beta$ -arrestin signaling, ERK and GSK3 $\beta$ ,<sup>2,4,27</sup> and compared this with receptor-mediated G protein signaling in the presence of BG, MG, or LG. Figure 6A shows a NT-induced time course of pERK phosphorylation in U2OS cells containing NTR1. The pERK signal peaks somewhat earlier in the presence of 4 nM NT (5 min) than with 10  $\mu$ M BG (10–15 min, Figure 6B), but the signals are nearly equal in magnitude. We thus measured pERK or pGSK levels by Western blot at 10 min, a time compatible with agonist or dye exposure activation, in the presence of BG, MG, LG, and various GPCRs (Figure 6C–F). U2OS/ $\beta$ -arrestin2-GFP cells expressing GPR35, NTR1, V2R, or no additional transfected receptor (control) were exposed to either 3 or 10  $\mu$ M BG, 10  $\mu$ M MG, or 10  $\mu$ M LG. In no instance did LG produce a change over basal for either pERK or pGSK. BG addition resulted in elevated pERK and pGSK in most instances, whereas MG produced a response profile intermediate between LG and BG.

#### Effect of Triphenylmethane Dyes on G Protein Related Signaling.

We also determined the effects of BG, MG, and LG on G protein signaling (Figure 7) using a bioluminescence apocalponin calcium reporter to assess Gq-protein signaling of the NTR1 and a bioluminescence resonance energy transfer cAMP, Gs reporter assay for the  $\beta$ 2AR and V2R. For the cAMP assay, we first determined that BG does not quench luciferin/luciferase luminescence (Figure 7A,B). Additionally BG, MG, and LG do not themselves activate cAMP signaling in cells expressing the  $\beta$ 2AR and V2R (not shown) or in cells with NTR1 and the apocalponin reporter (Figure 7E). In contrast to pERK and pGSK responsiveness to BG and MG, their preincubation with cells at greater than 3  $\mu$ M blocked neurotensin related Ca<sup>2+</sup> responsiveness and V2R and  $\beta$ 2AR cAMP signaling (Figure 7C,D,F). LG had no effect on signaling. Thus, taken together, the results are in agreement with a generalized biased effect of triphenylmethane dyes on signaling; with a preservation of  $\beta$ -arrestin (clathrin scaffolding) compatible pERK/pGSK based signaling and a concomitant loss of G protein signaling capability.

#### Binding of Malachite Green to $\beta$ -Arrestin2 Complexes.

In order to assess whether the observed activity of the triphenylmethane dyes on  $\beta$ -arrestin behavior could result from a direct interaction, we incubated HEK-293 cell lysates containing  $\beta$ -arrestin2-GFP fusion protein or GFP with nonfluorescent agarose beads containing a high affinity, single chain antibody against GFP (Figure 8). Following incubation of the beads with Malachite Green, by confocal microscopy the  $\beta$ -arrestin2-GFP beads demonstrated binding of the dye (Figure 8A,B) relative to the GFP control (Figure 8C,D) or beads not exposed to GFP (Figure 8E,F). Analysis of SDS-PAGE protein gels (Figure 8H) and Western blots (Figure 8I) of eluted beads confirmed that the predominant proteins isolated from the respective lysates were  $\beta$ -arrestin2-GFP and GFP.

## DISCUSSION

Thousands of metric tons of triphenylmethane dyes are used annually as colorizers.<sup>28</sup> Importantly, triphenylmethane dyes have a long safety record for use in humans as topical antibiotics, and newborns with purple, triple-dye stained umbilical cords have experienced their use in a medical setting.<sup>29–31</sup> While the antibacterial, antiphagocytic properties of triphenylmethane dyes were assessed more than 80 years ago,<sup>32</sup> only recently has BG

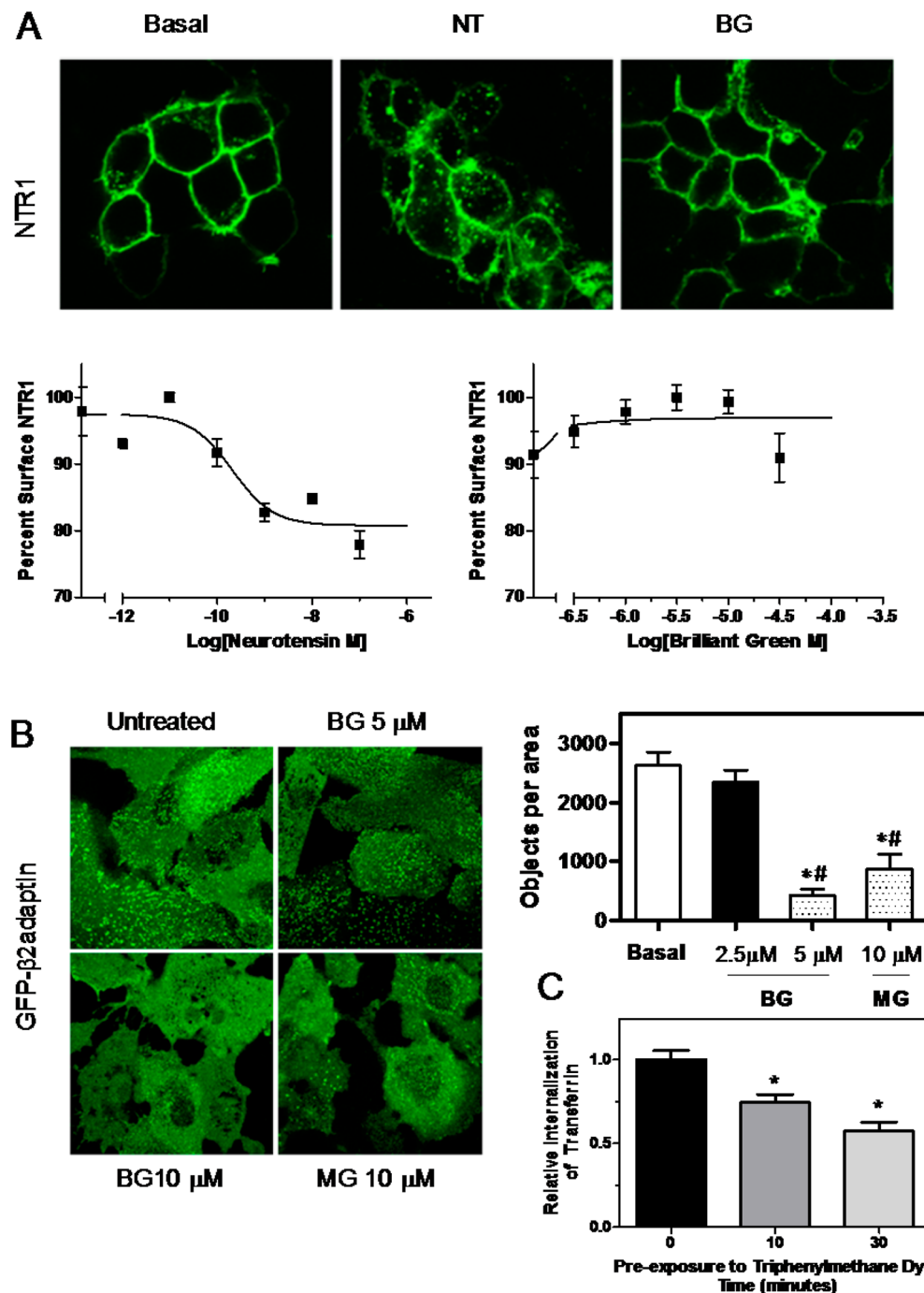


**Figure 5.** Triphenylmethane dye and endosome incorporation of adaptor proteins. (A) (Receptor/plasma membrane) HEK-293 cells in clear MEM expressing transiently transfected NTR1-GFP were treated with either 5 nM neurotensin peptide or 5 μM BG for 40 min at 37 °C, fixed, and confocally imaged. In the middle panels are shown graphical plots of an on-cell Western analyses of HA-NTR1 U2OS cells that demonstrate concentration-dependent ligand induced change of plasma membrane receptor after 40 min of NT or Brilliant Green treatment ( $N = 2$ ). (B) (AP2 complex/clathrin) HEK-293 cells that permanently express GFP-β2-adaptin were treated in clear MEM with vehicle, BG, or MG for 40 min at 37 °C and then fixed. GFP containing fluorescent puncta representing AP2 complexes in clathrin coated vesicles were imaged at 488 nm excitation and quantified as for β-arrestin-GFP. Data in the graph are mean  $\pm$  SEM and assessed in GraphPad Prism by one-way Anova using Bonferroni's post test (\* vs basal, # vs 2.5 μM BG,  $p < 0.05$ ,  $N = 4$ ). (C) (Transferrin) Transferrin internalization in U2OS cells in the presence of BG/MG was compared to cells not pretreated with triphenylmethane dye. The graph represents grouped data for cell types (with or without overexpressed NTR1, which showed similar responsiveness) and are presented as mean  $\pm$  SEM. Differences in internalized transferrin were assessed by Anova as above (\* vs basal,  $p < 0.05$ ,  $N = 2$ ).

been proposed as an antibacterial additive for gloves and in mouthwash for immune-compromised individuals.<sup>29,33</sup> Triphenylmethane dyes redistribute within cell membranes and are known to interact with cell receptors,<sup>34–36</sup> enzymes,<sup>37–39</sup> and DNA.<sup>30,40,41</sup> In some cases, the reported affinity is quite high, for

instance, with the *Torpedo californica* nicotinic acetylcholine receptor (AChR) the dissociation constant of crystal violet is 10 nM.<sup>35</sup>

The bioactivity of these dyes with their resulting economic benefits has resulted in their continued widespread environ-

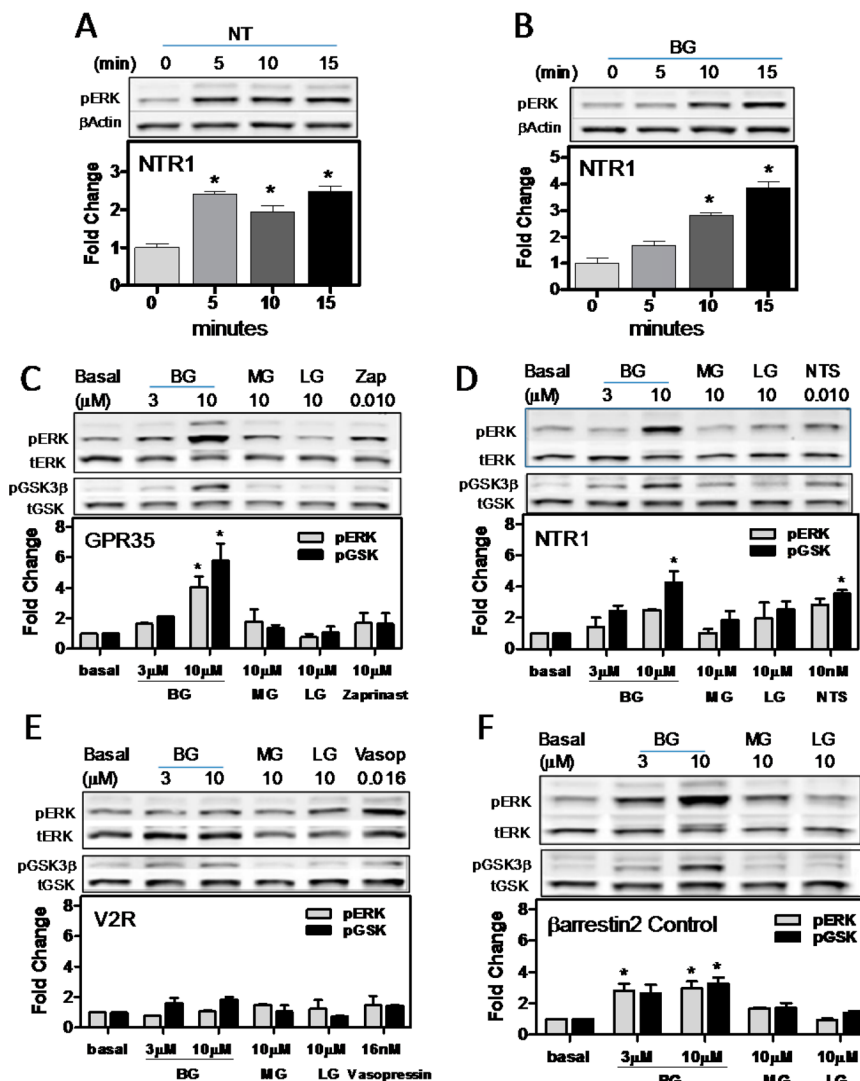


**Figure 6.** Effect of triphenylmethane dyes on ERK and GSK3 $\beta$  signaling. (A, B) Time course of pERK response in U2OS cells permanently expressing the NTR1 and  $\beta$ -arrestin-GFP treated with either 4 nM NT or 10  $\mu\text{M}$  BG. (C–F) U2OS cell lines permanently expressing GPR35, NTR1, V2R, or no transfected receptor ( $\beta$ -arrestin2 control) were treated with the indicated concentrations of BG, MG, LG, or cognate peptide for 10 min at room temperature. Phospho-ERK, total ERK, phospho-GSK3 $\beta$ , and total GSK3 $\beta$  were measured as described in Methods. Results are from  $N = 2$ –4 experiments and data are presented as mean  $\pm$  SEM. Data in the graphs were analyzed in GraphPad Prism using one-way Anova and Dunnett's post test against basal (\* corresponds to vs basal,  $p < 0.05$ ).

mental use. Malachite green is still considered the gold standard for aquaculture both as an antibiotic and antiparasitic based upon its relatively good efficacy and relatively low toxicity,<sup>14,42,43</sup> and solutions containing malachite green are readily available for the treatment of ornamental fish. However, it is the proven efficacy of these dyes and their low costs for treating consumable pond-raised fish of commercial importance, where effective alternatives are generally lacking, that drives their continued usage.<sup>30,42</sup> This has persisted despite toxicity concerns arising from their extended retention and metabolism in animal tissue and concerns over mutagenicity and carcinogenicity from either the dyes themselves or toxic byproducts such as LG. The concomitant legal restrictions in Europe and the U.S. has led to their ban in foods in many countries.<sup>30,43,44</sup> In comparison to the concerns about their long-term genetic effects, relatively little is known about the short-term, immediate effects of triphenylmethanes on cell biochemistry, in particular via GPCR signaling.

Our data show the triphenylmethane dyes MG and BG in low micromolar to sub-micromolar concentrations affect G protein-

coupled receptor signaling in cells within minutes of their application. Surprisingly, the two major legs of GPCR signaling seem to be oppositely impacted with G protein responses being reduced as shown in Figure 7 and  $\beta$ -arrestin consistent activation maintained, Figure 6. Importantly, even though BG increases ERK phosphorylation, multiple mechanisms may be at work, and a direct connection with  $\beta$ -arrestin binding remains to be established. Likewise, while the suppression of G protein-mediated GPCR signaling may be related to binding or activation of  $\beta$ -arrestins by these dyes, it is unclear whether alternative interactions are also in play. To address these issues, it will minimally be necessary to examine ERK activity in  $\beta$ -arrestin knockdown cells to determine the full extent to which  $\beta$ -arrestins contribute to observed BG/MG ERK signaling. While the concentration range of the dyes that we employed is compatible with that deemed safe to treat fish over brief to extended periods,<sup>30</sup> the immediate effects on G protein and  $\beta$ -arrestin signaling pathways that we observed may potentially explain

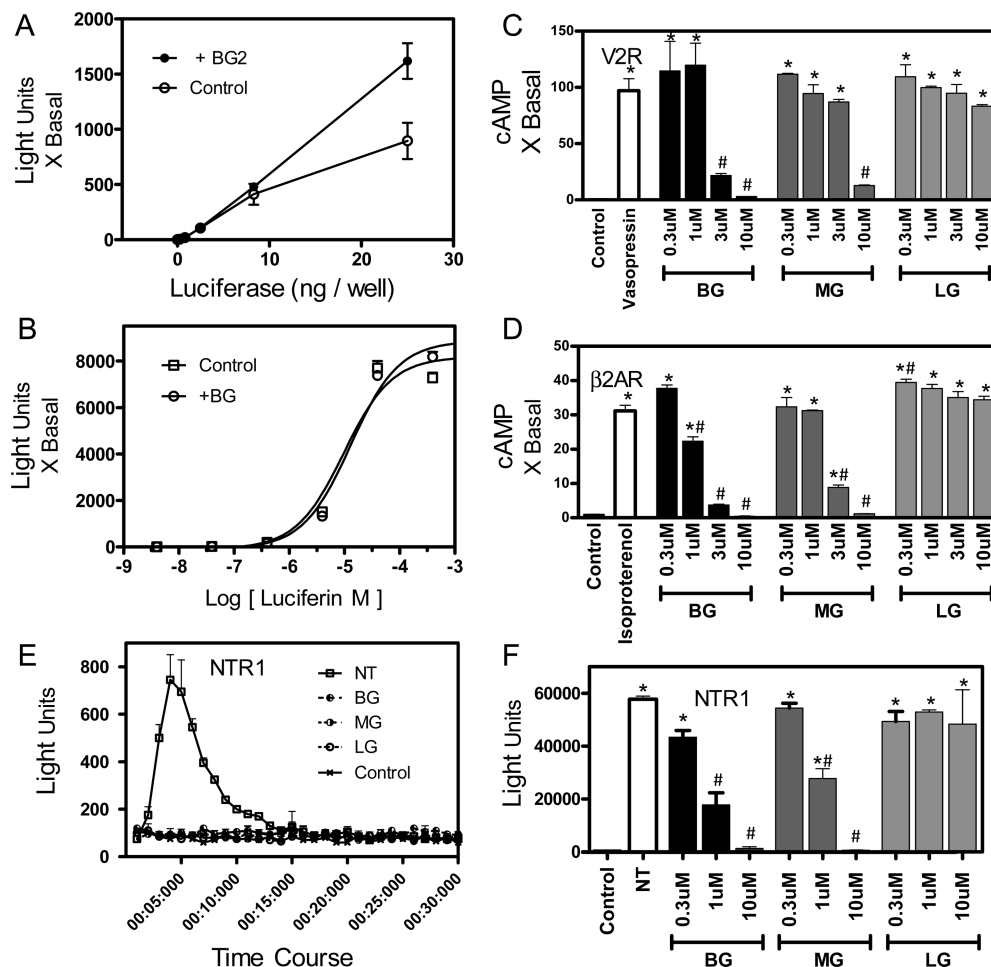


**Figure 7.** Effect of triphenylmethane dyes on receptor-mediated G protein signaling. (A) The linearity of the enzymatic cleavage of 1 mM luciferin by an increasing concentration of luciferase in a solution at room temperature was evaluated in the presence and absence of 10 μM BG ( $N = 2$ ). (B) Using a 2.5 ng/well concentration of luciferase as determined from (A), the dose response of luciferin in a solution at room temperature was measured in the presence and absence of 10 μM BG ( $N = 2$ ). (C, D) Measurement of cAMP in HEK-293 cells transiently transfected with either the V2R or β2AR was determined. Cells were pretreated for 10 min with the indicated concentrations of vehicle, BG, MG, or LG and then the cognate peptide, 16 nM vasopressin, or 10 μM isoproterenol was added. Cell cAMP was measured 10 s after agonist addition using the GloSensor bioluminescence assay in 96-well plates. Data were reported as mean  $\pm$  SEM. (E) HEK-293 cells transfected with the NTR1 and an apo-aequorin calcium reporter were exposed to vehicle, 10 nM neurotensin (NT) peptide, 10 μM BG, 10 μM MG, or 10 μM LG, and the time course of the aequorin luminescence was measured. Data are plotted as mean  $\pm$  SEM ( $N = 2$ ). (F) HEK-293 cells expressing the NTR1 were pretreated as in (C, D) and the calcium response measured with the apo-aequorin reporter ( $N = 2$ ). Data in the graphs C, D, F were analyzed in GraphPad Prism using one-way Anova and Bonferroni's post test (\* vs basal, # vs agonist,  $p < 0.05$ ).

some of the longer term cytotoxic behaviors of triphenylmethane dyes.<sup>45</sup>

There are no small molecule nonreceptor ligands available to modulate β-arrestin behavior, whose receptor-mediated activation results in receptor cargo moving to clathrin coated pits. This trafficking is normally a direct result of three processes: (1) self-interaction between the β-arrestin N- and C-termini with the exposure of C-terminal motifs governing; (2) an interaction with clathrin; and (3) an interaction with the AP2 adaptor complex in the presence of receptor.<sup>1</sup> However, a report of a C-terminal β-arrestin2 mutant with increased affinity for AP2 indicated that β-arrestin localization to clathrin coated pits can occur independently of receptor activation and that receptor cargo is necessary for the accumulation of AP2 in newly formed clathrin coated vesicles.<sup>46</sup> Recent studies also suggest that receptors as cargo are not passive passengers and can also modify the dynamics of clathrin coated pits.<sup>47</sup> Indeed, our data show that overexpression of NTR1s induce formation of additional clathrin

coated pits, potentially explaining the receptor/cell line efficacy differences observed for β-arrestin activation by BG/MG. Likewise, our BG/MG data pharmacologically recapitulate the behavior of the β-arrestin2 mutant,<sup>46</sup> demonstrating that in the presence of cognate receptor antagonists, activated β-arrestin2-GFP can bind clathrin without also being bound to activated cargo.

BG/MG treatment resulted in a loss of vesicular and aggregated GFP-β2adapton affecting endocytosis in general as indicated by the rapid reduction in transferrin internalization we observed. This suggests that AP2 in the presence of a β-arrestin with an intact β-adaptin binding motif may also require the presence of an activated receptor to properly incorporate in the clathrin scaffolds that drive vesicle formation. The triphenylmethane dyes potentially block otherwise active receptors from occupying clathrin-related sites by filling them with activated β-arrestin2 sans cargo. While the mechanism underlying BG/MG β-arrestin activation requires further study, a parsimonious

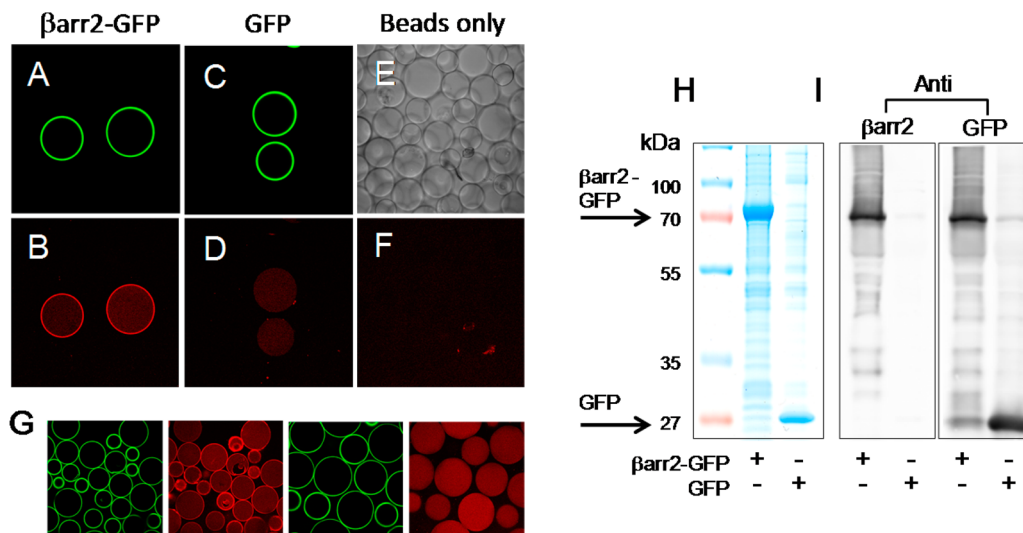


**Figure 8.** Interaction of Malachite Green with  $\beta$ -arrestin2-GFP coated anti-GFP beads. GFP-Trap agarose beads were exposed to lysates of HEK-293 cells transfected with  $\beta$ -arrestin2-GFP (A, B), lysates of HEK-293 cells transfected with GFP (C, D), or not exposed to GFP protein (control) (E, F). The beads were next treated with 10  $\mu$ M MG for 30 min at room temperature, washed, and imaged with a Zeiss LSM-510 confocal microscope at 20 $\times$ . GFP was assessed in the 488 nm channel and malachite green in the 633 nm channel. For comparative purposes, images of  $\beta$ -arrestin2-GFP, GFP, and control beads at the same wavelength were acquired and printed under identical settings. (A)  $\beta$ arr2-GFP exposed beads imaged for GFP. (B)  $\beta$ -Arrestin2-GFP exposed beads imaged for malachite green. (C) GFP exposed beads imaged for GFP. (D) GFP exposed beads imaged for malachite green. (E) Phase images of GFP-Trap control beads. (F) Control beads imaged for malachite green following treatment. (G) Panels from left to right depicting results from a different experiment showing a larger sample size of  $\beta$ -arrestin2-GFP exposed beads (leftmost two panels) and GFP exposed beads (rightmost two panels). GFP-Trap agarose beads eluted with SDS sample buffer were processed for SDS-PAGE. (H) Shown is an AcquaStain protein gel of  $\beta$ -arrestin2-GFP and GFP containing cell lysates from purification by GFP-Trap beads. (I) Corresponding Western blots of  $\beta$ -arrestin2-GFP and GFP lysates probed by antibodies to  $\beta$ -arrestin2 (left gel) and antibodies to GFP (right gel). Upper and lower arrows indicate expected positions at which each protein should run. Results are representative of 2–3 independent experiments. GFP in this figure corresponds to the variant S65T-GFP.

explanation is that a  $\beta$ -arrestin-scaffolded protein or  $\beta$ -arrestin itself is directly targeted by triphenylmethane dyes, GPCRs having no direct involvement. This is supported by the Malachite Green, bead, cell lysate studies; the receptor antagonist experiments, and the observation that cargo can indirectly effect clathrin coated-pit expression. Further studies with purified  $\beta$ -arrestin-GFP preparations may validate this hypothesis, perhaps verifying that  $\beta$ -arrestin contains a MG binding site using either mutagenesis or by exploiting the fluorescent enhancement of MG that can occur upon protein binding. This property of MG currently serves as the basis for a recently developed, cell-based MG reporter assay of protein dynamics.<sup>17</sup>

Our studies indicate that triphenylmethane dyes can be employed as tool compounds to study  $\beta$ -arrestin activity. The ability of triphenylmethane dyes to directly regulate processes involving  $\beta$ -arrestin trafficking and scaffolding may provide novel strategies to dissect the biological importance and clinical utility of this signaling pathway given the recent interest in biased medicinal compounds able to discriminate between receptor conformations favoring G protein or  $\beta$ -arrestin signaling.<sup>5,48</sup> Even without identifying the  $\beta$ -arrestin-related MG/BG target, it may be possible to develop compounds with better pharmacological properties based upon our finding differences between the potencies and efficacies of BG and MG for  $\beta$ -arrestin2 activation. Substantial numbers of triphenylmethane dyes are currently available for structure activity relationship (SAR) determinations. In fact, some dyes are already being evaluated for therapy of central nervous system disorders, such as Alzheimer's, that are characterized by abnormal plaque formation and believed associated with protein endocytosis.<sup>36,49–52</sup>

Triphenylmethane dyes, despite concerns about their cytotoxicity and environmental impact, continue to find roles as therapeutic tools. BG and MG can safely treat fish for extended periods against bacteria, fungus, and parasites that are refractory to other forms of drug therapy and most recently, Brilliant Blue variants have been investigated for the treatment of plaque forming diseases of the central nervous system. Our data taken together with these other studies suggest the effectiveness of triphenylmethane dye treatment may be due in part to their ability to disrupt clathrin-mediated endocytic trafficking, including inhibiting the entry of proteins, organisms, or obligatory nutrients into cells. If so, it may also be useful to examine the utility of triphenylmethane dyes as topical inhibitors of receptor mediated viral entry into cells, such as for HIV/CCR5, in instances where other methods are uneconomical, unavailable, or impractical.

## ASSOCIATED CONTENT

### S Supporting Information

Images illustrating clathrin/flag- $\beta$ -arrestin colocalization resulting from Malachite Green treatment are found in supplemental Figure S1. The effects of receptor overexpression on basal clathrin coated pit formation is shown in supplemental Figure S2. This material is available free of charge via the Internet at <http://pubs.acs.org>.

## AUTHOR INFORMATION

### Corresponding Author

\* (L.S.B.) L.Barak@cellbio.duke.edu; (M.G.C.) Marc.Caron@dm.duke.edu. Phone: 919-684-6245, 919-684-4533.

**Funding**

This work was supported by NIH Grants MH089653 to L.S.B. and DA029925 to (M.G.C., L.S.B.). We would also like to acknowledge the institutional support of the Duke University Comprehensive Cancer Center (WC). J.C.S. is a recipient of an F32 National Research Service Award (NRSA) 5F32MH092013-03.

**Notes**

The authors declare no competing financial interest.

**ABBREVIATIONS**

$\beta$ 2-adaptin, beta-adaptin 2 subunit of AP2;  $\beta$ -arrestin2, beta-arrestin 2;  $\beta$ 2AR, beta-adrenergic receptor 2; BG, Brilliant Green; GFP, green fluorescent protein; GPCR, G protein-coupled receptor; GPR35, G protein-coupled receptor 35; LG, Leukomalachite Green; MG, Malachite Green; NT, neurotensin; NTR1, neurotensin receptor 1; V2R, vasopressin receptor 2

**REFERENCES**

- (1) Gurevich, V. V., and Gurevich, E. V. (2006) The structural basis of arrestin-mediated regulation of G-protein-coupled receptors. *Pharmacol. Ther.* 110, 465–502.
- (2) Gurevich, E. V., and Gurevich, V. V. (2006) Arrestins: ubiquitous regulators of cellular signaling pathways. *Genome Biol.* 7, 236.
- (3) Shenoy, S. K., and Lefkowitz, R. J. (2005) Seven-transmembrane receptor signaling through beta-arrestin. *Science's STKE: Signal Transduction Knowledge Environ.* 2005, cm10.
- (4) DeWire, S. M., Ahn, S., Lefkowitz, R. J., and Shenoy, S. K. (2007) Beta-arrestins and cell signaling. *Annu. Rev. Physiol.* 69, 483–510.
- (5) Kenakin, T. (2012) The potential for selective pharmacological therapies through biased receptor signaling. *BMC Pharmacol. Toxicol.* 13, 3.
- (6) Barak, L. S., Ferguson, S. S., Zhang, J., and Caron, M. G. (1997) A beta-arrestin/green fluorescent protein biosensor for detecting G protein-coupled receptor activation. *J. Biol. Chem.* 272, 27497–27500.
- (7) Ferguson, S. S., Downey, W. E., 3rd, Colapietro, A. M., Barak, L. S., Menard, L., and Caron, M. G. (1996) Role of beta-arrestin in mediating agonist-promoted G protein-coupled receptor internalization. *Science* 271, 363–366.
- (8) Hershberger, P., Hedrick, M., Peddibhotla, S., Maloney, P., Li, Y., Milewski, M., Gosalia, P., Gray, W., Mehta, A., Sugarman, E., Hood, B., Suyama, E., Nguyen, K., Heynen-Genel, S., Vasile, S., Salaniwal, S., Stonich, D., Su, Y., Mangravita-Novo, A., Vicchiarelli, M., Smith, L. H., Roth, G., Diwan, J., Chung, T. D. Y., Caron, M. G., Thomas, J. B., Pinkerton, A. B., Barak, L. S. (2012) Small Molecule Agonists for the Neurotensin 1 Receptor (NTR1 Agonists), in *NCBI/Bookshelf/Probe Reports from the Molecular Libraries Program*, <http://www.ncbi.nlm.nih.gov/books/NBK47352/>.
- (9) Chong, C. R., Chen, X., Shi, L., Liu, J. O., and Sullivan, D. J., Jr. (2006) A clinical drug library screen identifies astemizole as an antimalarial agent. *Nat. Chem. Biol.* 2, 415–416.
- (10) Oakley, R. H., Laporte, S. A., Holt, J. A., Barak, L. S., and Caron, M. G. (2001) Molecular determinants underlying the formation of stable intracellular G protein-coupled receptor-beta-arrestin complexes after receptor endocytosis. *J. Biol. Chem.* 276, 19452–19460.
- (11) Azmi, W., Sani, R. K., and Banerjee, U. C. (1998) Biodegradation of triphenylmethane dyes. *Enzyme Microb. Technol.* 22, 185–191.
- (12) Oplatowska, M., Donnelly, R. F., Majithiya, R. J., Glenn Kennedy, D., and Elliott, C. T. (2011) The potential for human exposure, direct and indirect, to the suspected carcinogenic triphenylmethane dye Brilliant Green from green paper towels. *Food Chem. Toxicol.* 49, 1870–1876.
- (13) Andersen, W. C., Turnipseed, S. B., Karbiwnyk, C. M., Lee, R. H., Clark, S. B., Rowe, W. D., Madson, M. R., and Miller, K. E. (2009) Multiresidue method for the triphenylmethane dyes in fish: Malachite green, crystal (gentian) violet, and brilliant green. *Anal. Chim. Acta* 637, 279–289.
- (14) Halme, K., Lindfors, E., and Peltonen, K. (2007) A confirmatory analysis of malachite green residues in rainbow trout with liquid chromatography-electrospray tandem mass spectrometry. *J. Chromatogr., B: Anal. Technol. Biomed. Life Sci.* 845, 74–79.
- (15) O'Toole, M., Lau, K. T., Shepherd, R., Slater, C., and Diamond, D. (2007) Determination of phosphate using a highly sensitive paired emitter-detector diode photometric flow detector. *Anal. Chim. Acta* 597, 290–294.
- (16) Stojanovic, M. N., and Kolpashchikov, D. M. (2004) Modular aptameric sensors. *J. Am. Chem. Soc.* 126, 9266–9270.
- (17) Szent-Gyorgyi, C., Schmidt, B. F., Creeger, Y., Fisher, G. W., Zabel, K. L., Adler, S., Fitzpatrick, J. A., Woolford, C. A., Yan, Q., Vasilev, K. V., Berget, P. B., Bruchez, M. P., Jarvik, J. W., and Waggoner, A. (2008) Fluorogen-activating single-chain antibodies for imaging cell surface proteins. *Nat. Biotechnol.* 26, 235–240.
- (18) Laporte, S. A., Oakley, R. H., Zhang, J., Holt, J. A., Ferguson, S. S., Caron, M. G., and Barak, L. S. (1999) The beta2-adrenergic receptor/beta-arrestin complex recruits the clathrin adaptor AP-2 during endocytosis. *Proc. Natl. Acad. Sci. U. S. A.* 96, 3712–3717.
- (19) Kapur, A., Zhao, P., Sharir, H., Bai, Y., Caron, M. G., Barak, L. S., and Abood, M. E. (2009) Atypical responsiveness of the orphan receptor GPR55 to cannabinoid ligands. *J. Biol. Chem.* 284, 29817–29827.
- (20) Barak, L. S., Salahpour, A., Zhang, X., Masri, B., Sotnikova, T. D., Ramsey, A. J., Violin, J. D., Lefkowitz, R. J., Caron, M. G., and Gainetdinov, R. R. (2008) Pharmacological characterization of membrane-expressed human trace amine-associated receptor 1 (TAAR1) by a bioluminescence resonance energy transfer cAMP biosensor. *Mol. Pharmacol.* 74, 585–594.
- (21) Zhao, P., Sharir, H., Kapur, A., Cowan, A., Geller, E. B., Adler, M. W., Seltzman, H. H., Reggio, P. H., Heynen-Genel, S., Sauer, M., Chung, T. D., Bai, Y., Chen, W., Caron, M. G., Barak, L. S., and Abood, M. E. (2010) Targeting of the orphan receptor GPR35 by pamoic acid: a potent activator of extracellular signal-regulated kinase and beta-arrestin2 with antinociceptive activity. *Mol. Pharmacol.* 78, 560–568.
- (22) Barak, L. S., Oakley, R. H., Laporte, S. A., and Caron, M. G. (2001) Constitutive arrestin-mediated desensitization of a human vasopressin receptor mutant associated with nephrogenic diabetes insipidus. *Proc. Natl. Acad. Sci. U. S. A.* 98, 93–98.
- (23) Zhang, J., Barak, L. S., Anborgh, P. H., Laporte, S. A., Caron, M. G., and Ferguson, S. S. (1999) Cellular trafficking of G protein-coupled receptor/beta-arrestin endocytic complexes. *J. Biol. Chem.* 274, 10999–11006.
- (24) Laporte, S. A., Miller, W. E., Kim, K. M., and Caron, M. G. (2002) beta-Arrestin/AP-2 interaction in G protein-coupled receptor internalization: identification of a beta-arrestin binding site in beta 2-adaptin. *J. Biol. Chem.* 277, 9247–9254.
- (25) Laporte, S. A., Oakley, R. H., Holt, J. A., Barak, L. S., and Caron, M. G. (2000) The interaction of beta-arrestin with the AP-2 adaptor is required for the clustering of beta 2-adrenergic receptor into clathrin-coated pits. *J. Biol. Chem.* 275, 23120–23126.
- (26) Marion, S., Oakley, R. H., Kim, K. M., Caron, M. G., and Barak, L. S. (2006) A beta-arrestin binding determinant common to the second intracellular loops of rhodopsin family G protein-coupled receptors. *J. Biol. Chem.* 281, 2932–2938.
- (27) Del'guidice, T., Lemasson, M., and Beaulieu, J. M. (2011) Role of Beta-arrestin 2 downstream of dopamine receptors in the Basal Ganglia. *Front. Neuroanat.* 5, 58.
- (28) Thetford, D. (2000) Triphenylmethane and Related Dyes, in *Kirk-Othmer Encyclopedia of Chemical Technology*, John Wiley & Sons, Inc., New York.
- (29) Bahna, P., Hanna, H. A., Dvorak, T., Vaporciyan, A., Chambers, M., and Raad, I. (2007) Antiseptic effect of a novel alcohol-free mouthwash: a convenient prophylactic alternative for high-risk patients. *Oral Oncol.* 43, 159–164.
- (30) Culp, S. J., and Beland, F. A. (1996) Malachite green: A toxicological review. *J. Am. Coll. Toxicol.* 15, 219–238.
- (31) Suliman, A. K., Watts, H., Beiler, J., King, T. S., Khan, S., Carnuccio, M., and Paul, I. M. (2010) Triple dye plus rubbing alcohol

- versus triple dye alone for umbilical cord care. *Clin. Pediatr. (Phila)* 49, 45–48.
- (32) Felton, L. D., and Dougherty, K. M. (1922) The organotropic, bacteriotoxic, and leucocytotropic actions of certain organic chemicals. *J. Exp. Med.* 36, 163–179.
- (33) Reitzel, R. A., Dvorak, T. L., Hachem, R. Y., Fang, X., Jiang, Y., and Raad, I. (2009) Efficacy of novel antimicrobial gloves impregnated with antiseptic dyes in preventing the adherence of multidrug-resistant nosocomial pathogens. *Am. J. Infect. Control* 37, 294–300.
- (34) Bussler, J., Cordes, A., Heineke, W., Dengler, R., and Krampf, K. (2001) Pentobarbital and brilliant green modulate the current response of recombinant rat kainate-type GluR6 receptor channels differentially. *Neurosci. Lett.* 312, 91–94.
- (35) Lurtz, M. M., and Pedersen, S. E. (1999) Aminotriarylmethane dyes are high-affinity noncompetitive antagonists of the nicotinic acetylcholine receptor. *Mol. Pharmacol.* 55, 159–167.
- (36) Takenouchi, T., Sekiyama, K., Sekigawa, A., Fujita, M., Waragai, M., Sugama, S., Iwamaru, Y., Kitani, H., and Hashimoto, M. (2010) P2 × 7 receptor signaling pathway as a therapeutic target for neurodegenerative diseases. *Arch. Immunol. Ther. Exp.* 58, 91–96.
- (37) Bullough, D. A., Ceccarelli, E. A., Roise, D., and Allison, W. S. (1989) Inhibition of the bovine-heart mitochondrial F1-ATPase by cationic dyes and amphipathic peptides. *Biochim. Biophys. Acta* 975, 377–383.
- (38) Doerge, D. R., Chang, H. C., Divi, R. L., and Churchwell, M. I. (1998) Mechanism for inhibition of thyroid peroxidase by leucomalachite green. *Chem. Res. Toxicol.* 11, 1098–1104.
- (39) Glanville, S. D., and Clark, A. G. (1997) Inhibition of human glutathione S-transferases by basic triphenylmethane dyes. *Life Sci.* 60, 1535–1544.
- (40) Bose, B., Motiwale, L., and Rao, K. V. (2005) DNA damage and G2/M arrest in Syrian hamster embryo cells during Malachite green exposure are associated with elevated phosphorylation of ERK1 and JNK1. *Cancer Lett.* 230, 260–270.
- (41) Mittelstaedt, R. A., Mei, N., Webb, P. J., Shaddock, J. G., Dobrovolsky, V. N., McGarrity, L. J., Morris, S. M., Chen, T., Beland, F. A., Greenlees, K. J., and Heflich, R. H. (2004) Genotoxicity of malachite green and leucomalachite green in female Big Blue B6C3F1 mice. *Mutat. Res.* 561, 127–138.
- (42) Alderman, D. J. (1985) Malachite Green: a review. *J. Fish Dis.* 8, 289–298.
- (43) Schuetze, A., Heberer, T., and Juergensen, S. (2008) Occurrence of residues of the veterinary drug malachite green in eels caught downstream from municipal sewage treatment plants. *Chemosphere* 72, 1664–1670.
- (44) Culp, S. J., Mellick, P. W., Trotter, R. W., Greenlees, K. J., Kodell, R. L., and Beland, F. A. (2006) Carcinogenicity of malachite green chloride and leucomalachite green in B6C3F1 mice and F344 rats. *Food Chem. Toxicol.* 44, 1204–1212.
- (45) Jang, G. H., Park, I. S., Lee, S. H., Huh, T. L., and Lee, Y. M. (2009) Malachite green induces cardiovascular defects in developing zebrafish (*Danio rerio*) embryos by blocking VEGFR-2 signaling. *Biochem. Biophys. Res. Commun.* 382, 486–491.
- (46) Burtey, A., Schmid, E. M., Ford, M. G., Rappoport, J. Z., Scott, M. G., Marullo, S., Simon, S. M., McMahon, H. T., and Benmerah, A. (2007) The conserved isoleucine-valine-phenylalanine motif couples activation state and endocytic functions of beta-arrestins. *Traffic* 8, 914–931.
- (47) Soohoo, A. L., and Puthenveedu, M. A. (2013) Divergent modes for cargo-mediated control of clathrin-coated pit dynamics. *Mol. Biol. Cell* 24, 1725–1734.
- (48) Barak, L. S., and Peterson, S. (2012) Modeling of bias for the analysis of receptor signaling in biochemical systems. *Biochemistry* 51, 1114–1125.
- (49) Thomas, R. S., Lelos, M. J., Good, M. A., and Kidd, E. J. (2011) Clathrin-mediated endocytic proteins are upregulated in the cortex of the Tg2576 mouse model of Alzheimer's disease-like amyloid pathology. *Biochem. Biophys. Res. Commun.* 415, 656–661.
- (50) Iwamaru, Y., Takenouchi, T., Murayama, Y., Okada, H., Imamura, M., Shimizu, Y., Hashimoto, M., Mohri, S., Yokoyama, T., and Kitani, H. (2012) Anti-prion activity of Brilliant Blue G. *PLoS One* 7, e37896.
- (51) Wong, H. E., Qi, W., Choi, H. M., Fernandez, E. J., and Kwon, I. (2011) A Safe, Blood-Brain Barrier Permeable Triphenylmethane Dye Inhibits Amyloid-beta Neurotoxicity by Generating Nontoxic Aggregates. *ACS Chem. Neurosci.* 2, 645–657.
- (52) Zhang, C., Jackson, A. P., Zhang, Z. R., Han, Y., Yu, S., He, R. Q., and Perrett, S. (2010) Amyloid-like aggregates of the yeast prion protein ure2 enter vertebrate cells by specific endocytotic pathways and induce apoptosis. *PLoS One* 5, e12529.